

A Hula-Hoop Energy-Harvesting System

C. H. Lu¹, Y. J. Wang¹, C. K. Sung¹, and Paul C. P. Chao^{2,3}

¹Department of Power Mechanical Engineering, National Tsing Hua University, Hsinchu 30013, Taiwan

²Department of Electrical Engineering, National Chiao Tung University, Hsinchu 30013, Taiwan

³Institute of Imaging and Biophotonics, National Chiao Tung University, Hsinchu 30013, Taiwan

This paper proposes a hula-hoop energy-harvesting system that integrates a hula-hoop motion transformer with an electromagnetic generator. The hula-hoop motion transformer converts the linear motion from environment, machinery, or even human body into rotational one under specifically designed dynamic conditions. Then, the system can generate power through electromagnetism after combining the electromagnetic generator with the rotational motion. The equations prescribing the relation between induced voltage and power for the system are derived according to Faraday's theory. Meanwhile, the physical model of energy-harvesting system is established and the governing dynamic equations are derived as well via the Lagrange's equations. Good agreement of induced voltage and power between theoretical and experimental results is obtained. The maximum power that the system can generate is approximately 5 mW when the frequency and amplitude of the external excitation are 8 Hz and 11.2 N, respectively.

Index Terms—Electromagnetic induction, energy-harvesting system, Faraday's theory, hula-hoop motion transformer.

I. INTRODUCTION

THE energy-harvesting systems have been widely studied by many researchers in recent years for the utilization, mainly, of powering sensors of portable devices. Three major types of generators are employed to scavenge power from vibrations of environment, machinery or even human body: (a) electrostatic, (b) electromagnetic, and (c) piezoelectric generators [1]. Lately, researchers utilize these energy-harvesting generators to combine with other portable electronic devices or sensors to generate power from human daily motions. However, the amount of power is limited due to the small magnitude of vibration that the generator can use to create power [2]. On the contrary, the unlimited rotational motion could be adopted to remove the restriction of traditional linear-motion generators [3].

Most of the electromagnetic generators produce electricity by relative motions between the permanent magnets and the coils. For example, electromagnetic vibro-generators produce electricity with moving permanent magnets as the armature and fixed coils as the stator [4]. Besides, Holmes [5] presented another way to generate the power via the axial rotations of permanent magnets. Three types of electromagnetic power generation systems in the range of microwatts to tens of watts are proposed by Arnold [6] as well. Sasaki *et al.* [7] showed a device installed on a human body and a car engine to generate power under both resonant and non-resonant excitations. Meanwhile, Spreemann *et al.* [8] presented a MEMS generator using the similar principle. These two devices demonstrated the occurrence of rotational motions due to translational oscillations. In addition, some researchers utilized the electromagnetic generators via the rotational motion to have the power with the high excitation frequencies [9]–[11]. Yoshitake *et al.* [12] proposed a device on

the basis of hula-hoop motion for the purpose of quenching machine vibration while harvesting electricity by electromagnetic generators. Accordingly, this paper proposes a hula-hoop energy-harvesting system that is activated under small frequencies and magnitudes dedicated to human-body motions.

The hula-hoop motion transformer that converted the translational motion into rotational one under specific dynamic conditions was presented in the authors' previous paper [13]. The physical model was first established by the inspiration of the relative motion between the hula hoop and the human body, which was followed by deriving the equations of motion via Lagrange's Method. The occurrence of hula-hoop motion, i.e., the hula hoop undergoes rotational motion, was investigated.

This work integrates the motion transformer studied previously with permanent magnets, coils, and the electric circuit to form an electricity-generating system. Both theoretical and experimental studies are conducted. The occurrence of hula-hoop motion is attained by numerical simulation under various frequencies and magnitudes of excitations. Meanwhile, a linear motor is configured to mimic the harmonic human-body motion and drive the electromagnetic generator with an attached eccentric mass to rotational motions in the experiment. The generated power and working region can then be observed and validated under various excitations and initial conditions of the main and free masses.

II. THEORETICAL ANALYSIS

The physical model of hula-hoop generator is presented in Fig. 1 [13]. The human body is considered as the main mass while the generator with the attached eccentric mass is taken as the free mass. The gravity of both masses is not considered in this work. The external excitation drives the main mass with reciprocations only in y -direction. Meanwhile, it is intended to allow the free mass in revolution. The equations of motion of the system are derived via Lagrange's method, as in

$$(M + m)\ddot{y} + mR_m(\ddot{\theta} \cos \theta - \dot{\theta}^2 \sin \theta) + c\dot{y} + ky = F \cos(\omega t) \quad (1)$$

Manuscript received February 21, 2011; accepted May 09, 2011. Date of current version September 23, 2011. Corresponding author: C. H. Lu (e-mail: d9533827@oz.nthu.edu.tw).

Color versions of one or more of the figures in this paper are available online at <http://ieeexplore.ieee.org>.

Digital Object Identifier 10.1109/TMAG.2011.2155636

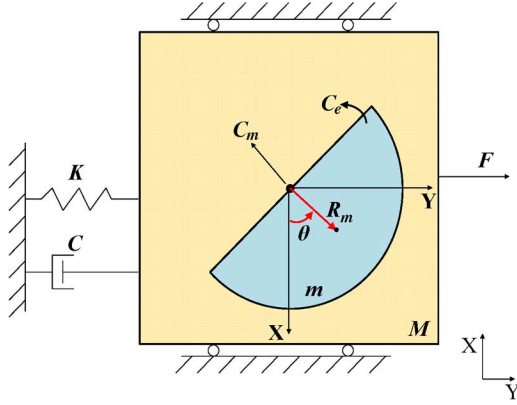


Fig. 1. Model of the hula-hoop generator.

and

$$(mR_m^2 + I) \ddot{\theta} + (c_m + c_e)\dot{\theta} = -mR_m\ddot{y} \cos \theta \quad (2)$$

where M , m , k , c , c_m , c_e , R_m , and F represent the main mass, free mass, spring rate, damping capacity of the damper, rotational damping due to the friction between the pin and hole, electrical induced damping, rotational radius between the center of the free mass and the pin, and the excitation force, respectively. θ is the angular displacement of the free mass. ω represents the excitation frequency, and I_{eq} is the moment of inertia of the free mass.

According to the Faraday's theory [14], the induced EMF voltage is equal to the negative rate of magnetic flux across a region enclosed by the coils. Thus, the EMF voltage can be described as

$$V = -N_c \frac{d\Phi}{dt} \quad (3)$$

where N_c is the number of coils and $d\Phi/dt$ indicates the magnetic flux linking the coils with respect to the time. From (3), the magnetic flux can be written as

$$\Phi = \int_s B \cdot ds = B_z A_c \sin(\theta) \quad (4)$$

that is in accordance with the rotational motion of the free mass under the variations from N-pole to S-pole. B means the magnetic field variation changed by the rotational velocity with $B(\theta) = B_z \sin(\theta)$; furthermore, B_z represents the magnetic field changed by the distance from each coil to the surface of magnet

$$B_z = \frac{B_0}{2} \left[\frac{M_h + (G_d + N_L \times d)}{\sqrt{M_r^2 + (M_h + G_d)^2}} - \frac{G_d + N_L \times d}{\sqrt{M_r^2 + (G_d + N_L \times d)^2}} \right] \quad N_L = 0, 1, 2, \dots \quad (5)$$

where B_0 is the remnant flux on the surface of magnet, M_h the height of the magnet, M_r the radius of the magnet, G_d the gap from surface of the magnet to the coil, and d the diameter of coil

wire. And N_L is the vertical turns of one coil, 30 turns in this research [14], [15], which can be shown as

$$N_L = \text{Int} \left(\frac{H_c}{d} \right) + 1 \quad (6)$$

where H_c and d are the height of one coil and the diameter of the coil wire, respectively. From (4), A_c presents the area enclosed by one coil; moreover, A_c changed by the radius of the surrounding coil can be shown as

$$A_c = \sum_{L_c=0}^{N_{Lc}} \pi(r_{in} + L_c \times d)^2 \quad L_c = 0, 1, 2, \dots, N_{Lc} \quad (7)$$

where N_{Lc} is the horizontal turns of one coil, 22 turns in this work, and then can be derived from

$$N_{Lc} = \text{Int} \left(\frac{r_{out} - r_{in}}{d} \right) + 1 \quad (8)$$

where r_{out} and r_{in} are the outer and inner radii of one coil, respectively. The rotational velocity is assumed to be a constant in this work, this makes $\theta = \omega_m t$; furthermore, the frequency of the induced voltage has the relation to the excitation frequency with $\omega_m = N_m \omega$ where N_m represents the pair of magnets [9]. Accordingly, the generator performs continuous revolutions, and the magnetic flux is assumed to be in a harmonic form in this work. Thus, the induced EMF voltage is presented as

$$V = -\beta N_c \frac{d\Phi}{dt} = -\beta N_c \left[\sum_{L=1}^{N_L} \sum_{L_c=1}^{N_{Lc}} A_c B_z \right] \omega_m \cos(\omega_m t) \quad (9)$$

where β , 0.59 in this work, is the geometrical factor including the effects of exact windings of each coil, gap from magnets to coils, and actual distribution of each magnetic flux [5], [8]. Then, we can have the induced rms voltage

$$V_{rms} = -\frac{1}{\sqrt{2}} \beta N_c \left[\sum_{L=1}^{N_L} \sum_{L_c=1}^{N_{Lc}} A_c B_z \right] \omega_m \quad (10)$$

Therefore, the output average power is given by

$$P = \frac{V_{rms}^2}{R_c + R_L} = \frac{\left\{ \beta N_c \left[\sum_{L=1}^{N_L} \sum_{L_c=1}^{N_{Lc}} A_c B_z \right] \omega_m \right\}^2}{2(R_c + R_L)} \quad (11)$$

where R_c and R_L are the coil resistance and load resistance, respectively.

III. NUMERICAL ANALYSIS AND EXPERIMENT

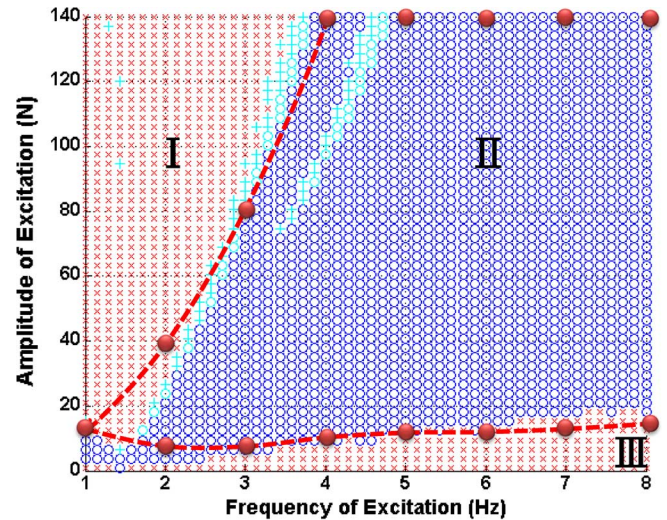
The system parameters are listed in Table I. Fig. 2 presents the region of occurrence of hula-hoop motion, which is obtained by numerical simulation based on the equations of motion. The factors that influence the occurrence of hula-hoop motion are the frequency and amplitude of the external excitation as well as the initial conditions, θ and θ' of the free mass. The zone featuring blue o's in Region II of Fig. 2 presents that the hula-hoop motion exists; on the contrary, the zones with red x's are where there

TABLE I
SYSTEM PARAMETERS AND INITIAL CONDITIONS (I.C.)

Symbol	Description	Value (Unit)
M	Main mass	5 kg
m	Free mass	0.063 kg
ϵ	Mass ratio ($m/(M+m)$)	0.0124
Rm	Rotational radius of free mass	0.0134 m
C	Damping ratio	0.12
K	Spring rate	411 N/m
c_m	Damping ratio of free mass	0.002
c_e	Electrical damping ratio of free mass	9.8446×10^{-6}
$y(0)$	I.C. of main mass	0 m
$y'(0)$	I.C. of main mass	0 m/sec
$\theta(0)$	I.C. of free mass	0 rad
$\theta'(0)$	I.C. of free mass	0 rad/sec
d	The diameter of the coil medal	0.11 mm
r_{out}	Outer radius of the entire coil	3.4 mm
r_{in}	Inner radius of the entire coil	0.95 mm
W_c	Width of the coil tracks	6.8 mm
H_c	Height of the coil tracks	3.17 mm
N_c	Number of coils	18
N_{LC}	Number of horizontal layers of coil	22
N_L	Number of vertical layers of coil	30
N_m	Number of magnet pairs	9
B_0	Remnant flux density of the permanent magnets (Nd-Fe-B)	1.14 T
R_c	Internal resistance	400 Ω
R_L	External resistance	1000 Ω

is no motion but with oscillations such as Region I and Region III. Meanwhile, the transition regions between Region I and Region II observed with cyan +’s shows the system works on reversal motions repeatedly. Note that the system in region II that is represented by the cyan o’s demonstrates hula-hoop motion at the transient state and oscillates with a different frequency. However, it becomes unstable at a steady state condition, i.e., no hula-hoop motion.

The experiment is carried out by using the linear motor to drive the hula-hoop energy-harvesting generator in Fig. 3. The linear-motor stage is utilized, herein, as the main mass for translational motions, which is constrained with two springs whose spring rate is listed in Table I to maintain oscillating about the middle position of the guide rail. The energy-harvesting generator with an attached eccentric mass made by copper, considered as the free mass of the system, is mounted on the linear-motor stage, and is also connected with a potentiometer to record the number of rotational turns of the generator. The motion of the linear-motor stage is controlled through a function generator with tunable frequency and amplitude. The designed generator with the diameter 6 cm, thickness 3 cm, and total weight 0.088 kg is shown in Fig. 4. The upper part of generator as the free mass has 18 magnets ($N_m = 9$) inserted and accompanied with an eccentric mass whose weight is 0.027 kg, and the lower part



	Blue (o)	Cyan (o)	Cyan (+)	Red (x)	Experimental Results Red (o)
Hula-hoop motion	Yes	No	No	No	Yes
Reversal	No	Yes	Yes	Yes	No

Fig. 2. Occurrences of hula-hoop motion obtained from direct numerical integration.

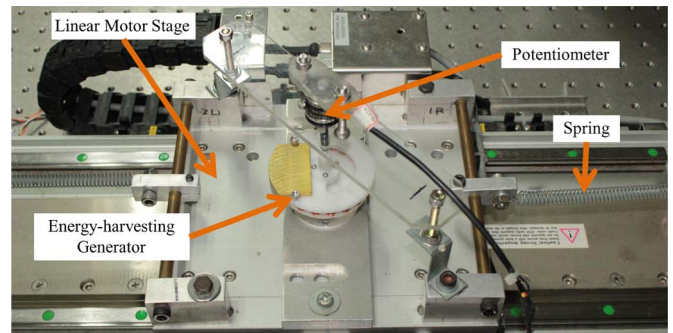


Fig. 3. Experimental setup of the hula-hoop energy-harvesting system.

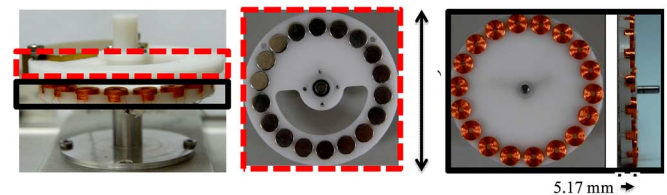


Fig. 4. Model of the hula-hoop energy-harvesting generator.

is accompanied with 18 coils. The results are observed via the oscilloscope.

Taking the excitation 5 Hz with the amplitude 24 N as an instance, Fig. 5(a) presents that the maximum induced EMF voltage 2.3 V with the frequency near 45 Hz. Meanwhile, Fig. 5(b) shows that the revolution of free mass recorded by the potentiometer is recognized as 5 Hz, same as the excitation frequency. Because of the periodic behavior of the free-mass revolutions, the induced voltage is observed only from 0 s to 0.1 s, as shown in Fig. 5(a). Besides, a small amount of phase

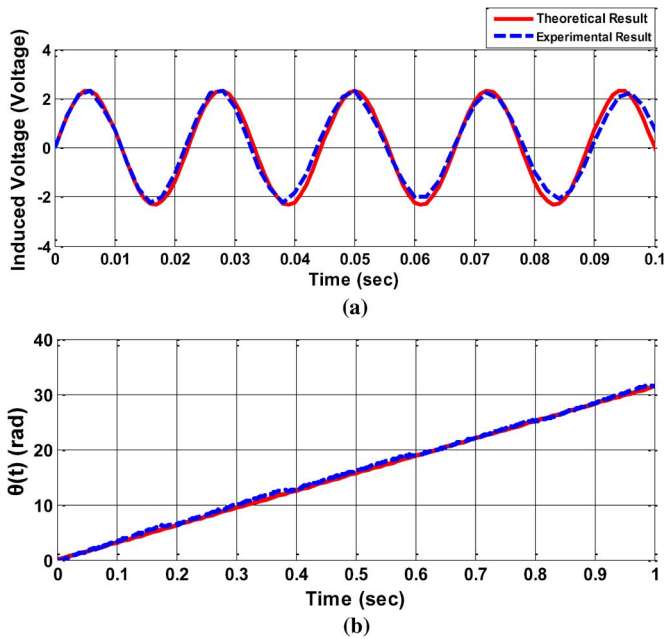


Fig. 5. (a) Induced EMF voltage by the generator. (b) Angular displacement of free mass (Excitation: 5 Hz, 24 N).

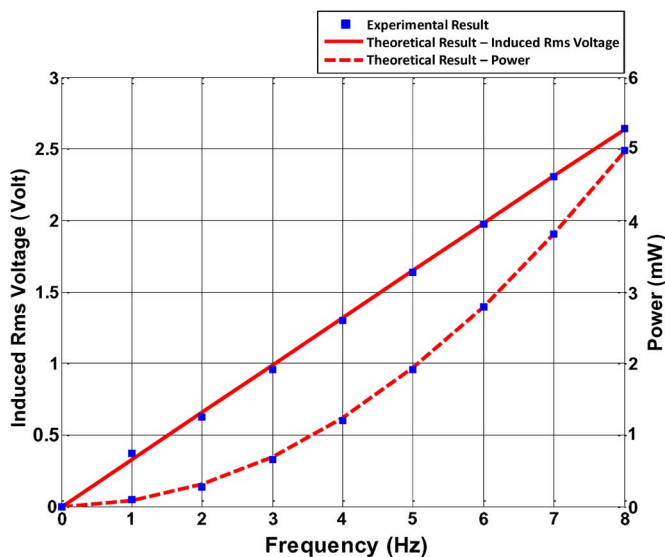


Fig. 6. Comparison between experimental and theoretical results for induced rms voltage and power (Excitation frequency: 0 Hz to 8 Hz).

difference is shown in Fig. 5(a) between the experimental and theoretical results because of the assembly error between the generator and the potentiometer, and also the unsteady voltage provided by the function generator. Furthermore, the response frequency of induced EMF voltage is 9 times the excitation frequency due to the alternate permutation from N-pole to S-pole for the magnets that have 9 pairs in this work.

Fig. 6 shows good agreement between the theoretical and experimental results for the induced voltage and power from excitation frequency 0 Hz to 8 Hz. The theoretical induced voltage depicted via red thick line is followed to increase by raising the excitation frequency, and so does the experiment featured with

blue square. Likewise, the power with red dotted line is also increased by increasing the excitation frequency theoretically, and the corresponding experimental results make the same trend as well. That proves the effectiveness of (9) which represents the equation of the induced voltage from the generator. The maximum generated power is approximately 5 mW when the excitation frequency and amplitude are 8 Hz and 11.2 N, respectively.

IV. CONCLUSION

A design of the hula-hoop energy harvesting system was conducted both theoretically and experimentally in this paper. The system is composed of a hula-hoop motion transformer and an electromagnetic generator. The physical model of the hula-hoop motion transformer was first established which was followed by dynamic analysis to find the range where the hula-hoop motion occurred under certain excitation and initial conditions. Furthermore, the equation of induced voltage for the electromagnetic generator was derived via Faraday's law. The induced rms voltage and power of the energy-harvesting generator were attained from both the experiment and numerical simulation; good agreement between them was obtained, which verified the effectiveness of the proposed design of the hula-hoop energy-harvesting system.

ACKNOWLEDGMENT

This work was supported in part by the National Science Council of Taiwan under Grant NSC 97-2221-E-007-050, and in part by the UST-UCSD International Center of Excellence in Advanced Bio-engineering sponsored by the Taiwan National Science Council I-RiCE Program under Grant NSC-99-2911-I-009-101.

REFERENCES

- [1] S. Roundy, P. K. Wright, and J. Rabaey, *Comput. Commun.*, vol. 26, pp. 1131–1144, 2003.
- [2] M. E. Hami, P. G. Jones, N. M. White, M. Hill, S. Beeby, E. James, A. D. Brown, and J. N. Ross, *J. Sens. Act. A*, vol. 92, pp. 335–342, 2001.
- [3] Y. J. Wang, C. D. Chen, and C. K. Sung, *J. Sens. Act. A*, vol. 159, pp. 196–203, 2010.
- [4] S. P. Beeby, R. N. Torah, M. J. Tudor, P. G. Jones, T. O'Donnell, C. R. Saha, and S. Roy, *J. Micromech. Microeng.*, vol. 17, pp. 1257–1265, 2007.
- [5] A. S. Holmes, G. Hong, and K. R. Pullen, *J. Microelectromech. Syst.*, vol. 14, pp. 54–62, 2005.
- [6] D. P. Arnold, *IEEE Trans. Magn.*, vol. 43, no. 11, pp. 3940–3951, Nov. 2007.
- [7] K. Sasaki, Y. Osaki, J. Okazaki, H. Hosaka, and K. Itao, *Microsyst. Technol.*, vol. 11, pp. 965–969, 2005.
- [8] D. Spreemann, Y. Manoli, B. Folkmer, and D. Mintenbeck, *J. Micromech. Microeng.*, vol. 16, pp. 169–173, 2006.
- [9] C. T. Pan and T. T. Wu, *J. Micromech. Microeng.*, vol. 17, pp. 120–128, 2007.
- [10] L. D. Liao, P. C.-P. Chao, J. T. Chen, W. D. Chen, W. H. Hsu, C. W. Chiu, and C. T. Lin, *IEEE Trans. Magn.*, vol. 45, no. 10, pp. 4621–4627, Oct. 2009.
- [11] P. C.-P. Chao, C. I. Shao, C. X. Lu, and C. K. Sung, *Microsyst. Technol.*, 2011, (In press).
- [12] Y. Yoshitake, T. Ishibashi, and A. Fukushima, *J. Sound Vib.*, vol. 275, pp. 77–78, 2004.
- [13] C. X. Lu, C. C. Wang, P. C. P. Chao, and C. K. Sung, *J. Vib. Acoust.*, vol. 133, 2009, (in press).
- [14] D. K. Cheng, *Field and Wave Electromagnetics*, 2nd ed. Reading, MA: Addison-Wesley, 1992, pp. 307–321.
- [15] N. Ida, *Engineering Electromagnetics USA*, 2000.